Enhance plasticity of bulk metallic glasses by geometric confinement

P. Yu, Y.H. Liu, G. Wang, H.Y. Bai,[a] and W.H. Wang
Institute of Physics, Chinese Academy of Sciences, Beijing 100080, China

(Received 23 June 2006; accepted 7 December 2006)

We report that bulk metallic glasses (BMGs) with large plasticity can be obtained in conventional brittle BMGs by a shrink-fit metal sleeve. The mechanical performance especially the plasticity in the $Zr_{41.2}Ti_{13.8}Cu_{12.5}Ni_{10}Be_{22.5}$ BMG with a shrink-fit copper sleeve is much enhanced. The approach results in the formation of the highly dense and frequent interacting and arresting events of shear bands and is the origin of the observed large global plasticity. The results present another simple step toward toughening the inherently brittle BMGs.

I. INTRODUCTION

The bulk metallic glasses (BMGs) have unique properties such as ultrahigh strength, lower Young's modulus, high elastic strain limit, excellent abradability, and corrosion resistance, which lead to outstanding application potentials in place of traditional crystalline metals.[1–3] However, the plasticity of BMGs at room temperature is usually disappointingly low due to the lack of dislocation systems and grain structure.[4–10] Upon yielding, the plastic deformation of the BMGs is highly localized into shear bands. These shear bands can rapidly propagate across the sample after their initiation and initiate cracking and lead to macroscopic catastrophic fracture. The limited global plasticity, less than 1%, restricts the use of BMGs as engineering materials.[4–10]

Cumulative efforts to improve the plastic deformability of BMGs have been shown to be effective in controlling the plastic instability.[11–23] A variety of BMG composites have been made by introducing the second crystalline phase or by in situ formation of crystalline phase through partial crystallization in the glassy matrix.[12–15] The ultimate aim of this approach is to restrict the rapid propagation of the shear bands by interaction with the ductile crystalline phases.[11–23] Recently, a few approaches have been proposed to successfully prepare the BMGs with large compressive plasticity,[16–24] such as to achieve a critical value of Poisson's ratio[22,23] or to introduce atomic-scale inhomogenities[10] or a phase-separated glassy structure.[24] However, the approaches are only focused on exploring new alloy systems and are not effective to the present numerous BMG systems. So, it would be beneficial to develop simple and feasible methods that could enhance the plasticity of the BMGs including the known BMG systems. On the other hand, unlike the crystalline materials, the mechanisms of the plastic deformation are well understood by motion of dislocations; the reason causing the plasticity in BMGs is unclear, and the relevant elucidations remain controversial.

The brittle materials, such as silicate glasses, are found to be sensitive to the surface structure and residual stress, which directly affect the ultimate plasticity and fracture.[25] Conventional silicate glasses have even greater problems with lack of ductility. Yet the strength of the silicate glasses can be increased by tempering to induce compressive residual stress at their surface. Therefore, they are widely used as structural materials (e.g., car windscreens, building glass windows) by using surface residual stresses to enhance their properties. Given the great current interest in improving the plasticity of BMGs, it is surprising that no attention has been paid to the analogous exploitation for these materials. Work[26,27] on residual stress in metallic glassy ribbons took place 15 to 20 years ago.

In this work, we report a feasible way using a shrink-fit metal sleeve to enhance the plasticity of the BMG. The idea is demonstrated for a $Zr_{41.2}Ti_{13.8}Cu_{12.5}Ni_{10}Be_{22.5}$ BMG (Vit1), and its compressive strain is markedly elevated by the shrink-fit metal sleeve. The reasons for the enhanced plasticity in the BMGs are discussed.

II. EXPERIMENTAL

Vit1 was fabricated by arc melting the pure elements in a vacuum and then suck casting into a Cu mold cooled by water. For the confined samples, a Cu sleeve with a

[a] Address all correspondence to this author.
e-mail: hybai@aphy.iphy.ac.cn
DOI: 10.1557/JMR.2007.0318

thickness of 0.5 mm and an external diameter 4 mm was first fixed in the Cu mold, and then the melted master alloy was sucked into the Cu sleeve. Three types of Cu-sleeve-wrapped Vit1 samples are prepared: sample A is a wrapped specimen, sample B is a loosely wrapped specimen, and sample C is a wrapped specimen whose sleeve is removed before the compressive test. The structure of the cylindrical alloys (cross-sectional surface and lateral surface) was characterized by x-ray diffraction (XRD) using a MAC M03 XHF diffractometer (Japan) with Cu K_α radiation. The cylindrical specimens of 3 mm in diameter and 6 to 8 mm in length were cut from the as-cast rods and tested under a uniaxial compressive deformation mode at room temperature using an Instron 5500R1186 machine (UK) with a loading strain rate of 5×10^{-4} s^{-1}. The specimen and the fracture surfaces after failure were investigated by scanning electron microscopy (SEM) using a Philips XL 30 SEM (Holland).

III. RESULTS AND DISCUSSION

The excellent glass-forming ability of the alloy facilitates easy manufacture of a glassy rod with a shrink-fit sleeve (the sleeve can be Cu, steel, Al and Ti alloys, etc.) by casting BMG-forming melt into the mold with the fixed sleeve. Figure 1(a) shows the Vit1 without and with a Cu sleeve. Figure 1(b) shows the XRD patterns of the core and the lateral surface of the wrapped Vit1 rod. The XRD as well as the thermal analysis carried out in a differential scanning calorimeter (not shown here) confirms the fully glassy structure of the sample. The SEM image in the inset of Fig. 1(b) shows that the Cu sleeve wraps the Vit1 perfectly, and no visible gaps at their interface are observed.

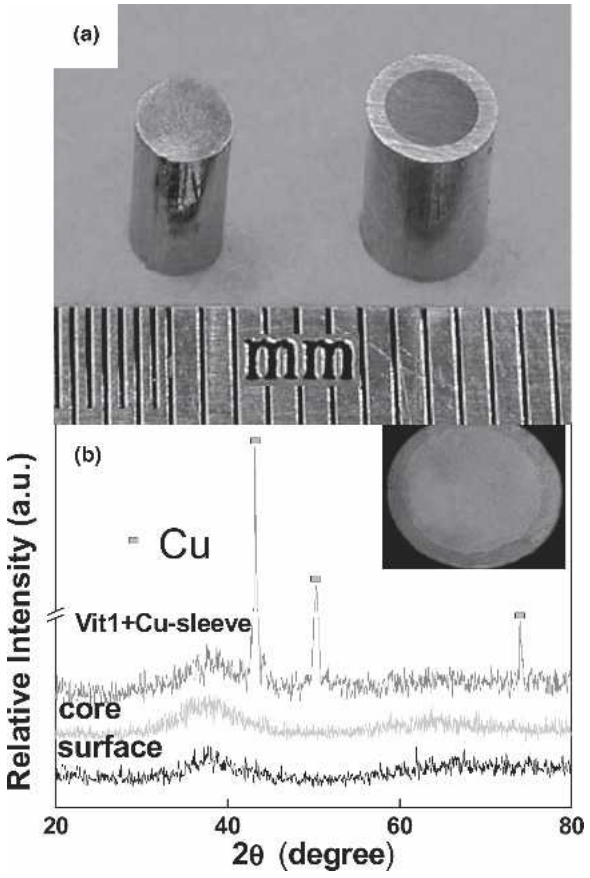

FIG. 1. (a) Vit1 and the Cu-wrapped Vit1. (b) XRD patterns of the Cu-wrapped Vit1; the inset is the SEM picture of the wrapped Vit1. The sharp crystalline XRD peaks are from the Cu sleeve.

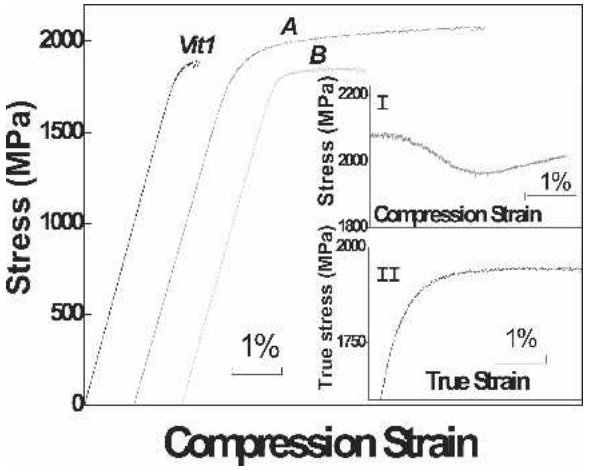

FIG. 2. Engineering stress–strain curves under compression for Vit1, the wrapped Vit1 rod A, and the loosely wrapped Vit1 rod B at a strain rate of 5×10^{-4} s^{-1}. Inset I: the stress–strain curve after 5% plastic strain of the wrapped Vit1 (the origin of the coordinate is 5% of plastic strain). Inset II: calculated true stress–strain curve of the wrapped Vit1.

Figure 2 shows the uniaxial compressive stress–strain curve of Vit1 and the wrapped Vit1 rods, and the data are summarized in Table I. The wrapped Vit1 (curve A) exhibits an elastic strain limit of 1.8% at a yield stress σ_y of ~1710 MPa, and the calculated elastic modulus E is 96.5 GPa, which are comparable to those of Vit1 without Cu sleeve (the σ_y, the elastic strain limit, and E are 1750 MPa, 1.8%, and 97.2 GPa, respectively, which are similar to that previously reported[2,3]). A significant

TABLE I. The room-temperature compressive test results for Vit1 and three types of Cu-sleeve-wrapped Vit1 samples.

Specimen	E (GPa)	σ_y (MPa)	σ_{max} (MPa)	ϵ_f (%)
Vit1	97.2	1750	1891	2.3
A	96.5	1710	2080	10.1
B	97.7	1690	1851	3.8
C	96.8	1715	1835	3.1

A, wrapped specimen; B, loosely wrapped specimen; C, wrapped specimen (sleeve removed before compression test).
E, Young's modulus; σ_y, yield stress; σ_{max}, maximum compression stress; ϵ_f, fracture strain.

plasticity of the wrapped Vit1 is exhibited in Fig. 2 after yielding, and the stress increases directly from yielding to 5% plastic strain and then displays a wavy behavior until the plastic strain reaches 8% where the fracture happened (see inset I of Fig. 2). The maximum compressive stress σ_{max} of the wrapped Vit1 is measured at 2080 MPa. Such a high plasticity has never been observed for Vit1 at room temperature, which shows a global plasticity of only ~0.5%.[12] The confined Vit1 can even resist a definite loading after fracture because the Cu sleeve still wraps the fractured sample, and the sample is further fragmentized and leads to a large serrated stress–strain curve after 8% strain. Therefore, the method makes the glass show some "fail-safe" behavior even though it is inherently brittle. The true stress–strain curve of the confined Vit1 is presented in inset II of Fig. 2. The flow stress gradually increases from yielding strength 1700 MPa to the maximum strength of 1950 MPa and then decreases slowly till fracture. The "work hardenability" in the glass is caused by the presence of the Cu sleeve. When the sleeve is removed from the wrapped Vit1 (specimen C), the Vit1 does not show any considerable plastic as listed in Table I. The lateral confinement does not affect the high elasticity of the alloy as shown in Fig. 2, which implies that the confinement mainly affects the plastic flow of the specimens. Therefore, the above results indicate that the method has markedly improved the plasticity and strength of the BMG. Such behavior could be exploited in many technological applications where BMGs or even other brittle materials are used, allowing these materials to be used in a more reliable way.

To understand the effect of the confinement, the lateral and the fracture surfaces of the fractured Vit1 are investigated by SEM. The fracture surface shows the typical veinlike pattern, as shown in Fig. 3(a). Figures 3(b) and 3(c) show the images of lateral surfaces of Vit1 and the confined Vit1 after fracture (the Cu sleeve was removed after compressive test), respectively. The lateral surface of Vit1 is very smooth, while the surface of the confined Vit1 is much rougher due to the rough inner surface of the Cu sleeve. The Cu sleeve has been treated by sanding and hydrofluoric acid corroding before casting, and the treatment makes its inner surface clean and rough, which leads to the convex surface of the sample and the mutual embedded interface of the two materials. The shear bands are visible on the surface of the two specimens [see Figs. 3(b) and 3(c)]. It can be clearly distinguished that the visible shear bands on the confined Vit1 surface are much denser than that of Vit1. Figure 4(a) shows the highly dense multiple shear bands near the ultimate fracture surface in the confined Vit1. The intershear band spacing is around 200 nm and the shear bands displaying wavy-passing patterns appear at various angles from the loading stress axis. This is clear in contrast with the typical images of unconfined Vit1, which fails catastrophically by the propagation of a single shear band under identical loading. A large number of multiple shear bands along the primary shear band dissipate the loading energy and delay the fracture. Figures 4(b)–4(d) present the typical subtle distribution of the shear bands in the surface of the confined Vit1. The surface picture reveals that the direction of the shear bands is distorted along the wavy lateral surface, and the shear bands are highly

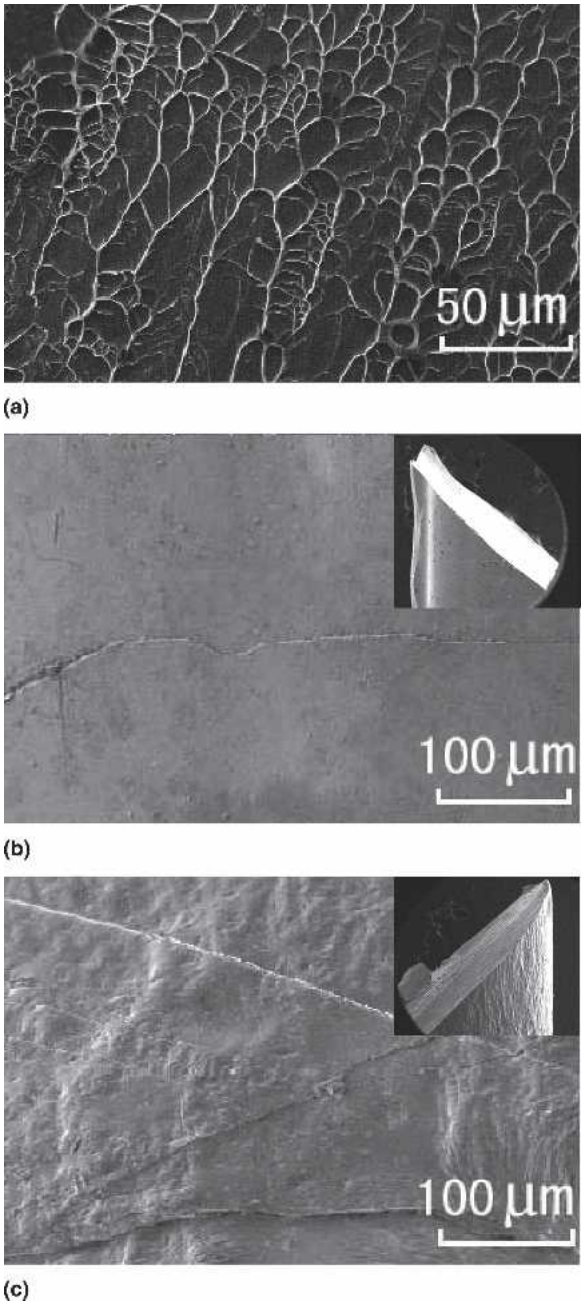

FIG. 3. (a) SEM picture of the fracture surface of the confined Vit1; (b) the lateral surface picture of fractured Vit1; and (c) the lateral surface of the confined Vit1 after shear fracture.

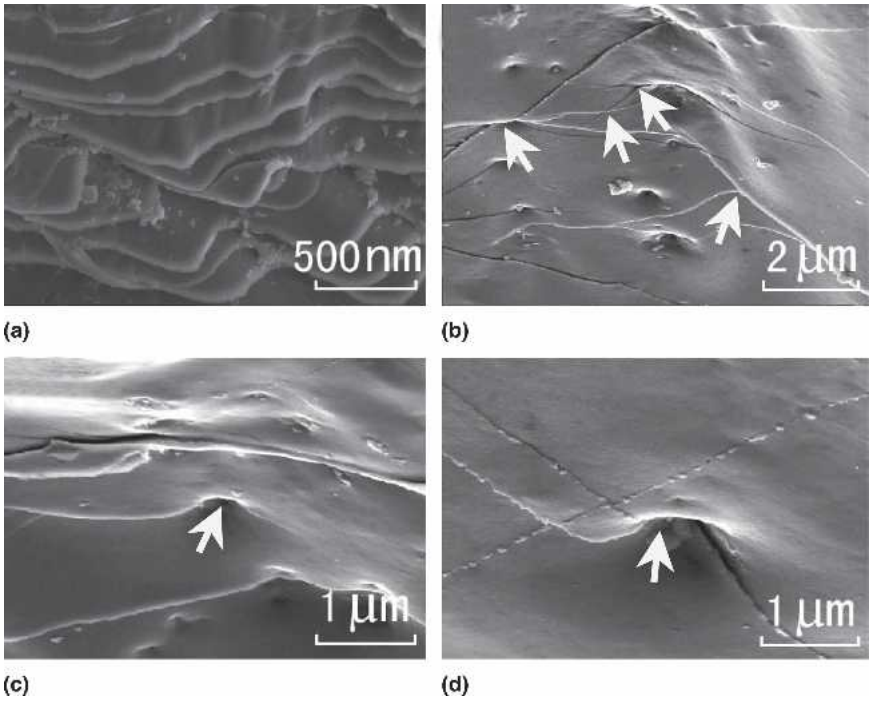

FIG. 4. SEM pictures show the shear bands on the confined Vit1 after shear fracture. (a) Near the fracture surface. (b) The subtle distribution of the shear bands, and the intersection of the shear bands are indicated by arrows. (c) The shear band is arrested by a convex point of the surface. (e) The shear band is branched by a convex point.

intersected and branched, and display wavy-passing patterns [Fig. 4(b)]. The intershear band spacing is estimated to be ~2 μm, which is much denser than that of Vit1 without confinement (~200 μm). The interactions of the shear bands in the confined Vit1 are more frequent. Figures 4(c) and 4(d) show the arrested and branched shear bands by the convex point of the surface. The shear bands are homogeneously distributed, and their interacting events take place all over the surface, which indicate that there is no significant localization of the shear bands. The highly dense and the frequent branching, interacting and intersecting shear bands induced by the confinement, which dissipate more loading energy, are attributed to the significant improvement of plasticity of the confined BMG.[16–21,28]

The key factors for the confining method are large differences in thermal expansion coefficient, Poisson's ratio, and elastic limit, and the mutual embedded interface between the BMG and the sleeve. Copper has a much larger coefficient of thermal expansion (CTE) 2.1×10^{-5} K^{-1} compared with that of Vit1[12] (8.5×10^{-6} K^{-1}). The smaller CTE of Vit1 is predicted to lead to less contraction compared with that of the Cu sleeve during cooling from the processing temperature. The mismatch of CTE between Cu and Vit1 causes the large thermal contraction of the sleeve and bulging of Vit1 during cooling process, which makes the sleeve wrap Vit1 tightly and a high surface compression.[29] On the other hand, copper is a typical metal with excellent plasticity but a small elastic limit (<0.2%), which is much lower than that of Vit1 (~2%). Thus, when compressing the wrapped Vit1 to its yielding limit, the Cu sleeve has been work hardened to above 200 MPa. Furthermore, due to the Poisson's ratio effect, both Vit1 and the Cu sleeve expand in the radial direction before failure under uniaxial compression. Since the Poisson's ratio of Cu (0.34) is lower than that of Vit1 (0.36^2), the Cu sleeve will expand less than Vit1 in the radial direction and also cause an increment in the confining pressure.[30] Therefore, the above factors result in the significant lateral confinement that supplies a compressive stress. The improved ductility comes from the fact that the ductile Cu effectively suppresses the runaway failure along a single shear band.

We note that the interface between the sample and the sleeve is crucial for the successful confinement. Curve B in Fig. 2 shows that for the loosely wrapped Vit1 sample with some gaps in the interface there is no obvious effect on the plastic improvement. The mutual embedded, intimate Vit1/sleeve interface can increase the contacting area between the sample and the sleeve and enhance the confining effect. The embedded interface can also induce more interactions of shear bands (branching, intersecting, and arresting). So, the confining method through introducing the confined stress and interface effect ultimately promotes the generation and the interaction of the shear bands throughout the bulk glass leading to excellent global plasticity.

IV. CONCLUSIONS

We find that the mechanical performance especially the plasticity in the $Zr_{41.2}Ti_{13.8}Cu_{12.5}Ni_{10}Be_{22.5}$ BMG with a shrink-fit copper sleeve is much enhanced by a shrink-fit metal sleeve. The approach results in the formation of the highly dense and frequent interacting and arresting events of shear bands that are the origin of the observed large global plasticity. The result presents another simple step toward toughening the inherently brittle BMGs and is applicable to broad brittle metallic glass alloys.

ACKNOWLEDGMENTS

We are grateful to D.Q. Zhao and M.X. Pan for the discussions. The financial support of the National Natural Science Foundation of China (Grant Nos. 50671117 and 50621061) is appreciated.

REFERENCES

1. A. Inoue, T. Zhang, and T. Masumoto: Al–La–Ni amorphous alloys with a wide supercooled liquid region. *Mater. Trans., JIM* **30,** 965 (1989).
2. W.H. Wang: Roles of minor additions in formation and properties of bulk metallic glasses. *Prog. Mater. Sci.* **52,** 540 (2007).
3. W.H. Wang, C. Dong, and C.H. Shek: Bulk metallic glasses. *Mater. Sci. Eng., R* **44,** 45 (2004).
4. F. Spaepen: A microscopic mechanism for study state inhomogeneous flow in metallic glass. *Acta Mater.* **25,** 407 (1977).
5. C.A. Schuh, A.C. Lund, and T.G. Nieh: New regime of homogeneous flow in the deformation map of metallic glasses: Elevated temperature nanoindentation experiments and mechanistic modeling. *Acta Mater.* **52,** 5879 (2004).
6. B. Yang, M.L. Morrison, P.K. Liaw, R.A. Buchanan, G. Wang, C.T. Liu, and M. Denda: Dynamic evolution of nanoscale shear bands in a bulk-metallic glass. *Appl. Phys. Lett.* **86,** 141904 (2005).
7. W.H. Jiang and M. Atzmon: The effect of compression and tension on shear-band structure and nanocrystallization in amorphous $Al_{90}Fe_5Gd_5$: A high-resolution transmission-electron-microscopy study. *Acta Mater.* **51,** 4095 (2003).
8. C.T. Liu, L. Heatherly, D.S. Easton, C.A. Carmichael, J.H. Schneibel, C.H. Chen, J.L. Wright, M.H. Yoo, J.A. Horton, and A. Inoue: Test environments and mechanical properties of Zr-base bulk amorphous alloys. *Metall. Mater. Trans. A.* **29,** 1811 (1998).
9. K.M. Flores and R.H. Dauskardt: Enhanced toughness due to stable crack tip damage zones in bulk metallic glass. *Scripta Mater.* **41,** 937 (1999).
10. W.I. Wright, R.B. Schwarz, and W.D. Nix: Localized heating during serrated plastic flow in bulk metallic glasses. *Mater. Sci. Eng., A* **319–321,** 229 (2001).
11. C. Fan and A. Inoue: Ductility of bulk nanocrystalline composites and metallic glasses at room temperature. *Appl. Phys. Lett.* **77,** 46 (2000).
12. R.D. Conner, R.B. Dandliker, and W.L. Johnson: Mechanical properties of tungsten and steel fiber reinforced $Zr_{41.25}Ti_{13.75}Cu_{12.5}Ni_{10}Be_{22.5}$ metallic glass matrix composites. *Acta Mater.* **46,** 6089 (1998).
13. U. Kühn, J. Eckert, N. Mattern, and L. Schultz: ZrNbCuNiAl bulk metallic glass matrix composites containing dendritic bcc phase precipitates. *Appl. Phys. Lett.* **80,** 2478 (2002).
14. Y.C. Kim, J.H. Na, J.M. Park, J.K. Lee, and W.T. Kim: Role of nanometer-scale quasicrystals in improving the mechanical behavior of Ti-based bulk metallic glasses. *Appl. Phys. Lett.* **83,** 3093 (2003).
15. C.C. Hays, C.P. Kim, and W.L. Johnson: Microstructure controlled shear band pattern formation and enhanced plasticity of bulk metallic glasses containing in situ formed ductile phase dendrite dispersions. *Phys. Rev. Lett.* **84,** 2901 (2000).
16. J. Das, M.B. Tang, K.B. Kim, R. Theissmann, F. Baier, W.H. Wang, and J. Eckert: "Work-hardenable" ductile bulk metallic glass. *Phys. Rev. Lett.* **94,** 205501 (2005).
17. G. Wang, Y.H. Liu, P. Yu, D.Q. Zhao, M.X. Pan, and W.H. Wang: Structural evolution of shear bands in work hardenable ductile bulk metallic glass. *Appl. Phys. Lett.* **89,** 251909 (2006).
18. J. Schroers and W.L. Johnson: Ductile bulk metallic glass. *Phys. Rev. Lett.* **93,** 255506 (2004).
19. W.H. Jiang, G.J. Fan, F.X. Liu, G.Y. Wang, H. Choo, and P.K. Liaw: Rate dependence of shear banding and serrated flows in a bulk metallic glass. *J. Mater. Res.* **21,** 2164 (2006).
20. H. Bei, S. Xie, and E.P. George: Softening caused by profuse shear banding in a bulk metallic glass. *Phys. Rev. Lett.* **96,** 105503 (2006).
21. Y.H. Liu, G. Wang, R.J. Wang, and W.H. Wang: Super plastic bulk metallic glasses at room temperature. *Science* **315,** 1385 (2007).
22. W.H. Wang: Correlations between elastic moduli and properties in bulk metallic glasses. *J. Appl. Phys.* **99,** 093506 (2006).
23. J.J. Lewandowski, W.H. Wang, and A.L. Greer: Intrinsic plasticity or brittleness of metallic glasses. *Philos. Mag. Lett.* **85,** 77 (2005).
24. J.C. Oh, T. Ohkubo, Y.C. Kim, E. Fleury, and K. Hono: Phase separation in $Cu_{43}Zr_{43}Al_7Ag_7$ bulk metallic glass. *Scripta Mater.* **53,** 165 (2005).
25. D.J. Green, R. Tandon, and V.M. Sglavo: Crack arrest and multiple cracking in glass through the use of designed residual stress profiles. *Science* **283,** 1295 (1999).
26. A.T. Alpas and J.D. Embury: Flow localization in thin layers of amorphous alloys in laminated composite structures. *Scripta Metal.* **22,** 265 (1988).
27. Y. Leng and T.H. Courtney: Fracture behavior of laminated metal-metallic glass composites. *Metall. Trans. A* **21,** 2159 (1990).
28. Y. Zhang, W.H. Wang, and A.L. Greer: Making metallic glasses plastic by control of residual stress. *Nat. Mater.* **5,** 857 (2006).
29. C.C. Aydiner, E. Ustundag, B. Clausen, J.C. Hanan, R.A. Winholz, M.A.M. Bourke, and A. Peker: Residual stresses in a bulk metallic glass-stainless steel composite. *Mater. Sci. Eng., A* **399,** 107 (2005).
30. W.N. Chen and G. Ravichandran: Dynamic compressive failure of a glass ceramic under lateral confinement. *J. Mech. Phys. Solids* **45,** 1303 (1997).